UNIVERSITY OF CALIFORNIA,

IRVINE

Effect of Simulated High Hydrogen Content Combustion Environments on Abradable Properties of Ceramic Turbine Coatings

THESIS

submitted in partial satisfaction of the requirements

for the degree of

MASTER OF SCIENCE

in Chemical Engineering & Materials Science

by

Madhura Basu Majumder

Thesis Committee:

Professor Daniel R. Mumm, Chair

Professor Mikael Nisson

Professor Lorenzo Valdevit

2015

DEDICATION

To

my husband Dr. Shoubhik Mukhopadhyay

for his encouragement

and my family for their belief in me

Table of Contents

LIST OF FIGURES

LIST OF TABLES

ACKNOWLEDGEMENT

I would like to express my deepest respect to my committee chair and my advisor, Professor Daniel R. Mumm, for his continuous support and motivation: he continually encouraged me and provided guidance in regard to research, and reinforced knowledge in regard to teaching. Without his supervision and persistent help this dissertation would not have been possible.

I would like to convey my regards to the thesis committee members, Professor Mikael Nilsson and Professor Lorenzo Valdevit, for their valuable time consumed guiding my research work and for the improvement of this thesis.

In addition, I would like to thank my colleagues and friends, especially Russell Clayton, Kliah Soto Leytan and Kara Phillips for their tremendous contribution in this project; thanks to the Chemical Engineering and Materials Science department for the constant assistance throughout this project.

I thank The Laboratory for Electron and X-ray Instrumentation (LEXI) for providing access to the high-tech equipment required for image analysis, and University of California Irvine for the academic help. I am thankful to be a part of this project financially supported by the Department of Energy as part of the Advanced Combustion Turbines Research Projects (FE0011929).

ABSTRACT OF THE THESIS

Effect of Simulated High Hydrogen Content Combustion Environments on Abradable Properties of Ceramic Turbine Coatings

By

Madhura Basu Majumder

Master of Science

University of California, Irvine, 2015

Professor Daniel R. Mumm, Chair

Air plasma sprayed (APS) abradable coatings are used in the turbine hot section to reduce the stator-rotor gap, minimizing gas leakage. These coatings are designed to exhibit controlled removal of material in thin layers when the turbine blades sweep through the coating, which protects the mechanical integrity of the turbine blade. In an effort to lower CO_2 emissions, high H_2 content fuel is being explored. This change in chemical composition of the fuel may affect the microstructure, abradability and durability of the coatings at turbine operational temperatures. The presence of high water vapor in the combustion chamber leads to accelerated degradation of the sacrificial coating materials. In this work, zirconia based composite materials with a machinable phase and varied porosity have been used to study microstructural evolution, thermal and chemical stability of the phases and abradable characteristics of baseline coating systems in both humid and dry environments. Investigation of the mechanisms that control the removal of materials and performance of abradable coatings through thermo-mechanical tests will be discussed.

INTRODUCTION

Coal is the most abundant resource of fuel available for power generation in the world; only in U.S. 39.3% of electricity generation was based on coal consumption in the year 2013. Although it is a cheap fuel source, it also produces a large amount of greenhouse gases contributing to global warming. Integrated Gasification Combined Cycle (IGCC) offers the possibility of using coal for power generation while reducing its impact on the environment.

The Department of Energy (DoE) provides research funding to support development of advanced turbine systems for use in IGCC combustion environments. Their combination contributes in the

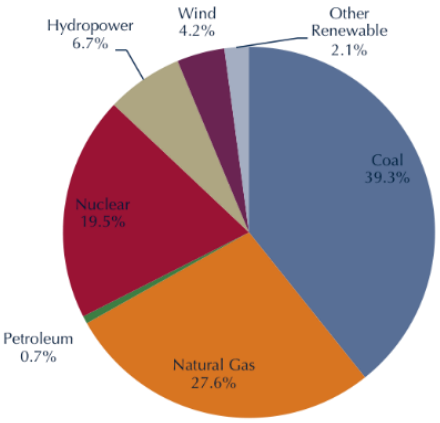

Fig. 1 Sources of U.S. greenhouse gas emissions (2013). (http://www3.epa.gov/)

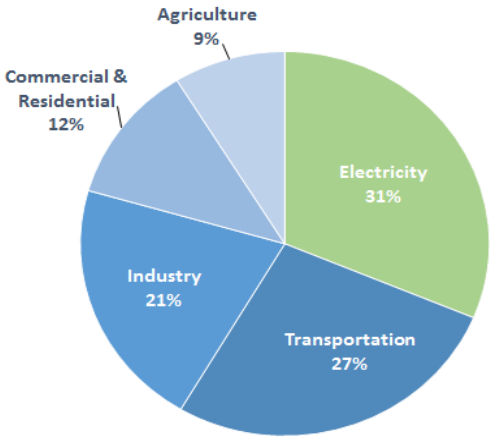

Fig. 2 U.S. Net Electricity Generation by Energy Source (2013) (http://www.c2es.org/)

power generation and reduces emission of CO_2, SO_2 and NOx using cleaner combustion fuel. IGCC uses a high-pressure gasifier to transform coal and other carbon based fuels into Synthetic

gas or syn gas ($CO+H_2$) and removes impurities (Carbon, Sulphur, particulate matter etc.) from the syn gas prior to the power generation cycle. Excess heat produced during the process is then passed to the steam turbine; which minimizes energy loss and emission, and reduces its operating cost.

The Clean Power Plan of August, 2015 by United States government set the limits of carbon emission by the power plants for the first time. This will add to the motivation of reducing greenhouse emission and overcoming the challenge of the installation cost.

Commercially used technologies such as pulverized coal (PC) and natural gas combined cycle (NGCC) plants typically clean exhaust after combustion. In IGCC operation, however, syn gas from the gasifier is cleaned before it is used as combustion fuel in the gas turbine. It is easier to clean high pressurized and more concentrated CO_2 from the syn gas produced from the

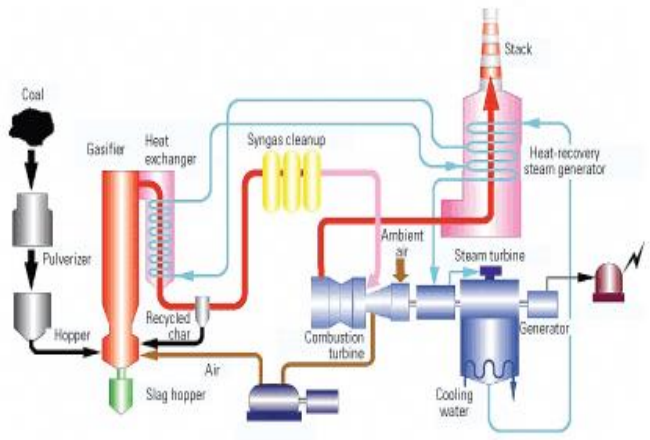

Fig. 3 Integrated Gasification Combined Cycle

(http://www.netl.doe.gov/)

gasification process. This allows for cleaner operation than power generation by current PC or NGCC combustion technology.

Syn gas is a mixture comprising of carbon monoxide, carbon dioxide, and hydrogen. The syn gas is produced by a gasification process of carbon containing fuel to a gaseous product that has some heating value. The syn gas may contain some trace elements of impurities, which are removed through further processing and either recovered or redirected to the gasifier. If the amount of nitric oxides is high in the syn gas, it must be separated to avoid production of acid rain and the risk of air pollution.

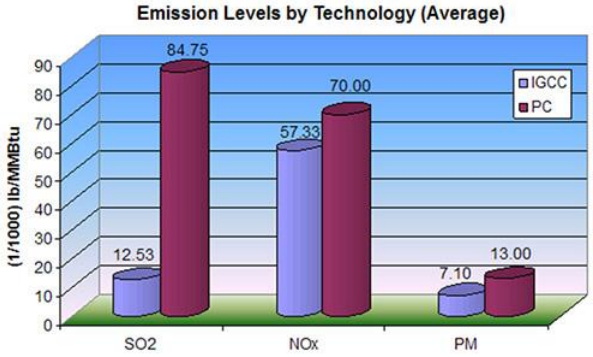

Fig. 4 Average emissions comparison for sulfur dioxide (SO2), nitrogen oxides (NOx), and particulate matter (PM) between IGCC and pulverized coal (http://www.netl.doe.gov/)

The biggest challenge for the turbine industry to replace the combustion fuel (from coal to syn gas) is that synthetic gas fuel will introduce a large volume of water vapor in the turbine inlet. The moisture contents will likely be in the range of 15-30 % depending on the amount of carbon-capture, fuel-to-air ratio and strategies for combustor dilution and component cooling (1). Therefore the primary concern is to study how the turbine components (blade, thermal barrier

coating, and abradable coatings) adapt to this almost 4-fold increase of humidity in the combustion chamber (typical range of moisture content is 7-8%).

As part of the Advanced Combustion Turbines Research (FE0011929) funded by the Department of Energy, this project '**Abradable Sealing Materials for Emerging IGCC-Based Turbine System**' investigates the effect of high hydrogen content combustion environment on the abradable materials system. These coating materials are comprised of a metal or ceramic matrix, a second phase incorporated to enhance machinability and are sprayed with polymer pore formers to create porosity in the coatings.

BACKGROUND

Abradable coating systems for high temperature gas turbines are considered to be the 'black art' in the turbine industry because the available information on these materials is very limited, even though it has been used since late 1960s. They are applied to help minimize the clearance distance between the rotating blade and the stator, and therefore reduce leakage in the gas path, leading to increases in efficiency and reductions in fuel consumption. There are a number of materials currently used as abradable systems for different parts of the turbines; commercially used system for compressor are Ni/Graphite and AlSi/hBN and MCrAlY/hBN/Polyester for turbine sections (2). When the turbine blades sweep through the coating the layered structure of these materials enhances removal of coating in thin layers and the compliant sacrificial coating protects the mechanical integrity of turbine blades.

Reviewing the literature available from late 70's it can be seen that the general concept has always been the same; with time the operational temperature range increased and so did the demand for more durable materials. In 1976, researchers used MCrAlY, a porous compliant base with controlled thermal conductivity, to improve the oxidation and erosion resistance. Rolls Royce patented Co/Ni-alloy coated glass particles to be used for plasma spraying gas turbine engine components and production of abradable seals; these exhibit relatively low thermal conductivity providing an effective thermal barrier and resistance to oxidation and thermal shock. GE, Rolls Royce and other turbine manufacturers wanted to design a protective layer with low thermal conductivity, high oxidation and erosion resistance which would minimize the back flow of gases protecting the blade tip.

Starting from only 4,000kW in 1939, the output of the industrial gas turbine has grown in size phenomenally, to around 250,000kW by the late 1990s and to over 510,000kW presently. Higher

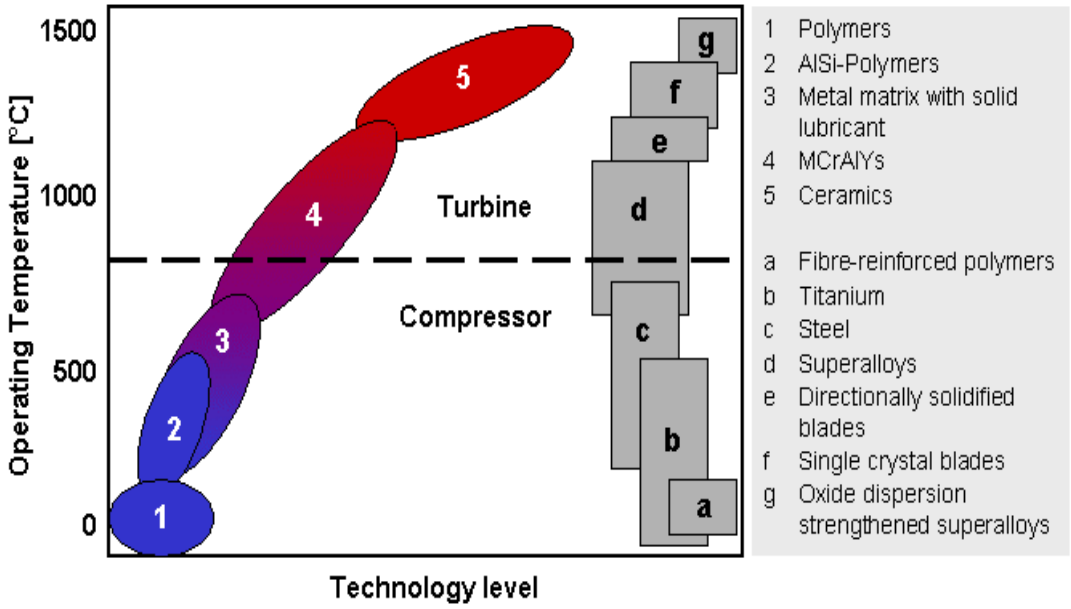

Fig. 5 Advancement of Technology level with increasing temperature (2)

efficiency is linked to the achievable turbine inlet temperatures (Carnot cycle); which led to many complicated schemes for cooling of the hot gas path components. But it was the combination of materials, thermal barrier coatings and cooling technologies that has made extremely high inlet temperature possible. When the world's first industrial turbine set, Neuchatel gas turbine power plant, was put into service in 1940 the operational conditions for the gas turbine cycle included a turbine inlet temperature of 550°C and pressure ratio of 4.2:1. It took Siemens 17 years to increase the inlet temperature by 266°C; and today the achievable inlet

temperature is about 1600°C. The massive increase of temperature called for rapid advancement of materials used; especially inside the high temperature zone.

From Fig. 5 it is clear that for temperatures above 1200°C ceramic materials should be used because of their high melting temperatures and very low thermal conductivities. Metallic superalloys (MCrAlY) are widely used as substrates on top of which the ceramic abradables are sprayed on, and therefore they must be compliant with each other.

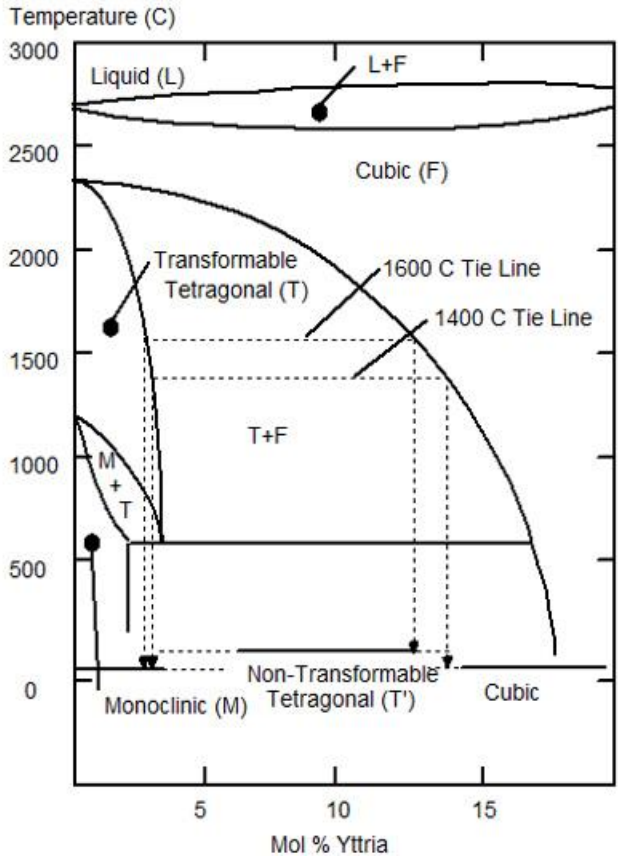

Fig. 6 Yttria stabilized Zirconia phase diagram

(http://www.azom.com/)

Zirconium oxide is the most extensively employed abradable material because its thermal expansion coefficient is very close to the expansion coefficient of MCrAlY superalloys (3). Zirconium oxide (ZrO_2) is used to make crucibles (as they can withstand very high temperature and thermal shock), to make furnace linings, foundry bricks etc. It is well known that ZrO_2 adopts a monoclinic crystal structure at room temperature and transitions to tetragonal and cubic phases with increasing temperatures. The volume expansion caused by the cubic to tetragonal to monoclinic transformation induces large stresses, and these stresses cause ZrO_2 to crack upon cooling from high temperatures. Dopants such as magnesium oxide (MgO), yttrium oxide (Y_2O_3, yttria) Fig. 6, calcium oxide (CaO),cerium (III) oxide (Ce_2O_3) are used to stabilize the tetragonal and/or cubic phases; the focus here will be on YSZ and Dysprosia stabilized Zirconia (DySZ).

Abradable materials should be both ‘soft’ enough to have good abradability and ‘hard’ enough to withstand the erosion by the gas stream at extremely high temperature and gas flow. To meet this complex combination of requirements these materials contain two or three different constituents. Yttria stabilized Zirconia (YSZ) or Dysprosia stabilized Zirconia (DySZ) ceramic matrix, a self-lubricating non-metal phase and/or some amount of pores. The matrix gives the strength, while controlled pores enable the fracture of the inter-particle bonding which help in clean cuts with minimum material transfer to the blade tip.

The solid lubricants, such as hexagonal Boron Nitride (hBN), Bentonite, etc. shear easily making the cut smoother and help to remove materials in layers instead of in large pieces. Hexagonal Boron Nitride consists of a layered structure comprising a network of $(BN)_3$ rings which makes it

an insulator with very different bonding in basal planes. The covalent bonding of the boron and nitrogen atoms in the same layer localizes the free electrons; different layers of hBN are bonded by weak van der Waals force that enables the layers to slide against each other. This is a useful property for a lubricant or releasing agent. Other significant properties of boron nitride, which in practice make them desirable at high temperatures, are its high-temperature resistance, thermal shock resistance, high-thermal conductivity, its chemical inertness, non-toxicity and environmental safety.

Ceramic abradable coatings are generally sprayed by Air Plasma Spray (APS) because material release, porosity and structural strength can be controlled with this process. There are many thermal spray processes, such as: plasma arc spray coating, high-velocity oxy-fuel coating (HVOF), flame spray coating, etc. Abradable coating materials are sprayed mainly using air plasma process which is illustrated in Fig. 7 Air Plasma Spray (APS) process diagram.

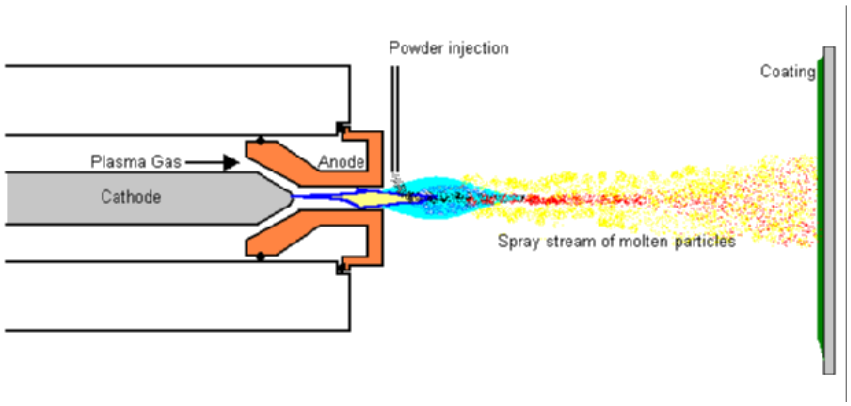

Fig. 7 Air Plasma Spray (APS) process diagram
(http://www.gordonengland.co.uk/)

The anode and the cathode sparks a very high temperature (>16000°K) plasma arc using the gas flowing through the electrodes. Typically helium (He), Hydrogen (H_2), Nitrogen (N_2) or a

mixture is ionized which initiates the plasma plume several centimeters in length. The feed stock injects the coating powders into the plasma jet, accelerated and impact on the surface of the substrate to form the coating.

Fig. 8 is shown here to emphasize the structure of as-sprayed materials. APS process sprays the molten or semi-molten composite powders onto the dense zirconia layer and forms layered pancake like structures mixed with pores. The weakening phase when melted starts creating a network around the YSZ grains.

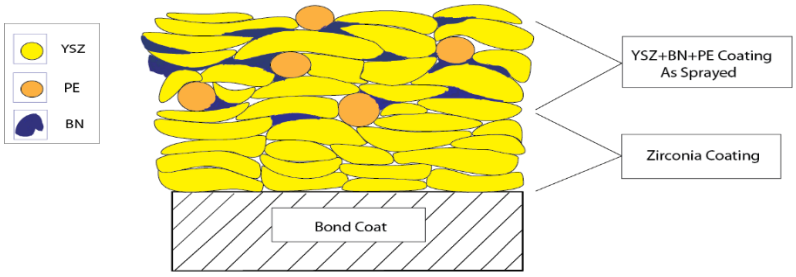

Fig. 8 Thermally sprayed composite material

Coating mechanics

The wear mechanisms of coatings (particularly metal superalloys) are rather complex including cutting, smearing, adhesive transfer, crushing, melting and tribo-oxidation (4). It has been found that porous coatings are sensitive to the incursion rate, rotational velocity and seal geometry (5). Engineering of abradable coatings is challenging because they have to be both soft enough to be abradable, as well as hard enough to be mechanically stable. It has been found that even with

similar hardness the abradability can be very different for different kind of coatings. In this report, the focus will only be on ceramic coatings failure mechanisms.

Zirconia abradable technology is essentially derived from the extensive thermal barrier coating base, where the use of partially/fully stabilized zirconia is rather well known for its excellent thermal shock resistance, toughness, and sintering resistance. The combination of low elastic modulus of zirconia (compared to other high temperature materials), high melting and sintering resistance, and the ability to be sprayed relatively thick (e.g., 2.0 mm) with suitable but controllable defect and macroporosity concentrations (e.g., pores and splat boundaries), all contribute to machinable coating structures that greatly assist in design against thermal shock damage.

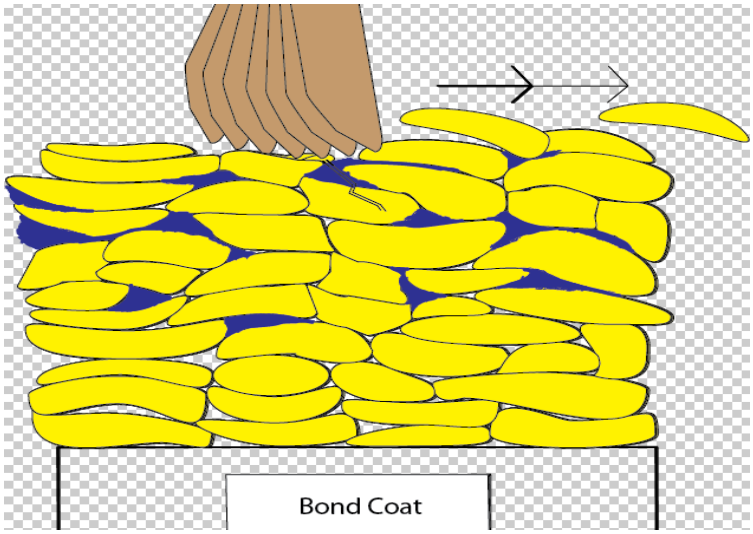

Fig. 9 Interaction between Turbine blade and the coating

The mechanism of cutting or wearing of a ceramic abradable at high speed in engine applications is accomplished by removal of small particle debris, typically less than 100 μm in size that

streams away with the gas flow (6). When the turbine blade first comes into contact with the abradable seal, the kinetic energy of the blade transfers to the coating in form of a compressive force. This force creates micro cracks perpendicular to the coating surface; ideally the stress built up on the crack tip should be released among the pores and the weakening phase (hexagonal boron nitride in this case) which would prevent any deformation in the coating.

In addition to initiating cracks the blade also eliminates material from the surface, resulting into a clean-cut surface, or an irregular one, depending on the particle size ejected, matrix bonding and material transfer. The best scenario would be removal of materials in layers instead of large debris; size of the particles must be small so that there would not be any risk of erosion later in the turbine stages from the interaction. Material transfer from the blade to the coating creates lumps on the surface which is somewhat necessary (since smoother surface is not desirable), but the opposite (coating->blade) is not a benign process.

In this project, the evolution of abradable coatings (for the hot section of turbine) in the presence of water vapor and the change in their properties have been investigated. The thesis will first explain the synthesis and preparation procedures of ceramic composite powders and then review the techniques required for the image analysis of the sintered pellets. After that the experiments and their results will be explained, in the end future goals will be discussed.

SYNTHESIS AND PREPARATION

Four different commercially available powders have been used for the microstructural study; Yttria stabilized Zirconia and two composites comprising Dysprosia stabilized Zirconia and Yttria stabilized Zirconia with polyester and Hexagonal Boron Nitride as the solid lubricant phase. Zirconia creates the matrix in all of these composites, Polyester (PE) burns out during the heat treatment process and creates large pores (average particle size is about 60 μm) and lastly the releasing agent (evenly distributed hexagonal Boron Nitride flakes) helps the coating to be more machinable during interaction with the turbine blade.

Table 1 Powders/composites used in this work

1)TZ8Y: Zirconium Oxide Yttrium Oxide	2)2460 NS: Zirconium dioxide Yttrium Oxide Polyester
3)Durabrade 2192: Zirconium Oxide Dysprosium Oxide Polyester Boron Nitride	4)Sultzer Metco 2395 Zirconium Oxide Yttrium Oxide Polyester Boron Nitride

Powders were first analyzed to check if they meet the specifications mentioned in the materials sheet and for contamination using x-ray diffraction technique. Powders were then ball-milled to achieve finer powders, which were pressed together and sintered using a tube/box furnace. After sintering, they were measured for density and hardness, and polished using metallography techniques to prepare them for image analysis in SEM.

X-ray diffraction

It is a technique to identify phases of a crystalline material and provide information on unit cell dimensions. Wavelength of X-rays is about 1Å (10^{-10} m) and it is comparable with the size of an atom.

When an incident beam of monochromatic X-rays hits the target material scattering X-rays away from atoms within the material; they undergo either constructive or destructive interference. This process is called X-ray diffraction. The diffraction of X-rays by crystals is described by Bragg's Law, **nλ= 2dsinϴ;** which explains the condition on ϴ [scattering angle] for the constructive interference to be maximum [n, **λ** and d represents a positive integer, wavelength of the beam and interplanar distance consecutively].

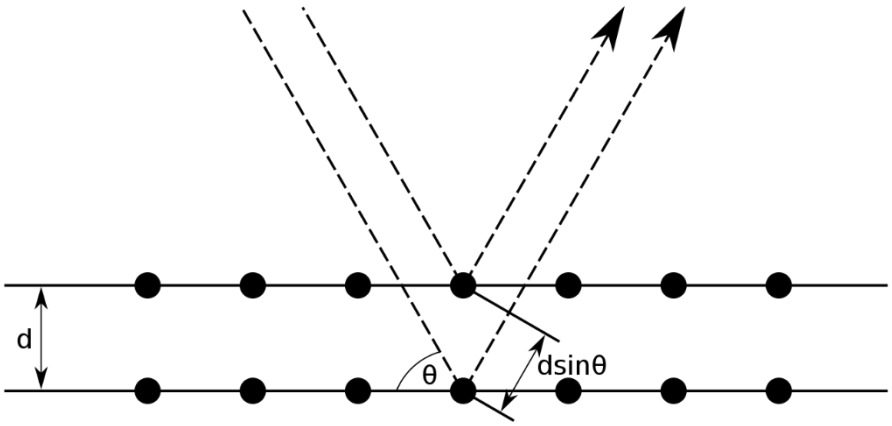

Fig. 10 Bragg Diffraction

(https://en.wikipedia.org/wiki/Bragg%27s_law)

The powders are not single crystals, but are composed of many small crystallites in all possible orientations. Thus when XRD is performed on powder materials, the diffraction pattern contains all possible interatomic planes. If the scattering angle changes systematically, every possible diffraction peaks could be detected.

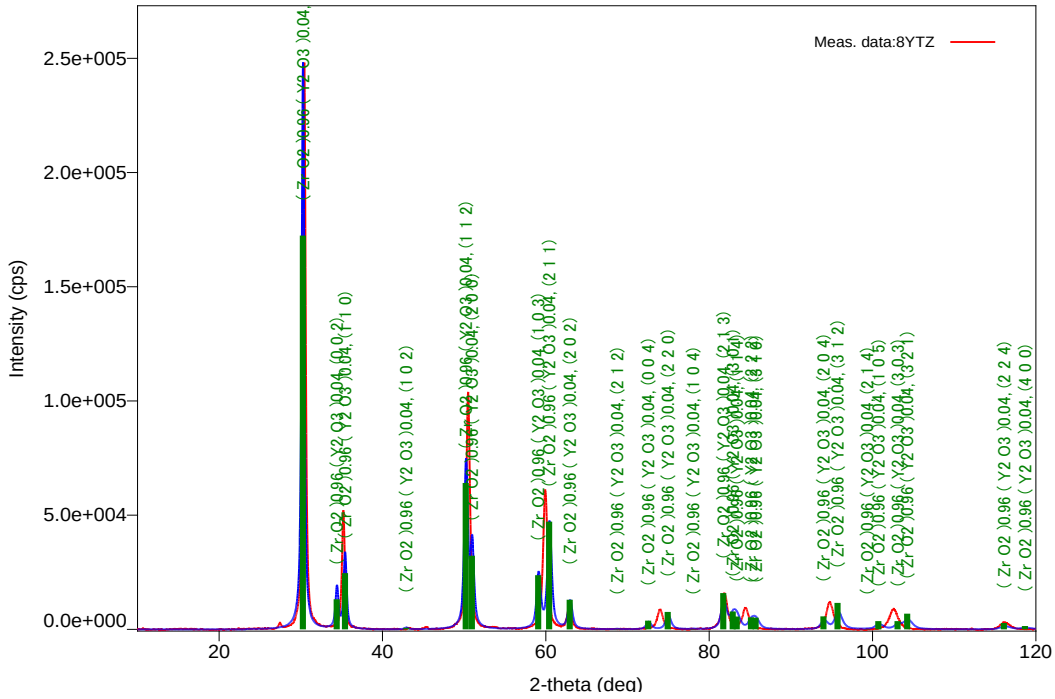

Fig. 11 XRD peaks of 4Y-TZP and 8YSZ

Here, homogenized and finely ground powder forms were used to determine the average bulk composition diffracting the x-rays by the atomic planes of the materials to confirm the agreement with the materials specification provided by the manufacturer and to verify their purity. Fig. 11 shows XRD of a 4Y-TZP (4 mol% yttria partially stabilized Zirconia) and 8YSZ.

Ball mill

To make more uniform and finer composition the powders were ball milled by mixing 150 gm media, 10 g powder and 80-100 ml de-ionized water in a bottle using 65 rpm speed for 24 hours. Powders were dried on a hot plate and ground back to powder form using porcelain mortar pestle.

Ball milling process was used to:

(a) break the agglomerates present in the composites.

(b) mix powders with organic binder so that they do not break while taking them out from the uniaxial press or Carver press.

(c) make an uniform mixture of TZ8Y and different amount of Polyester to vary porosity in the sintered pellet.

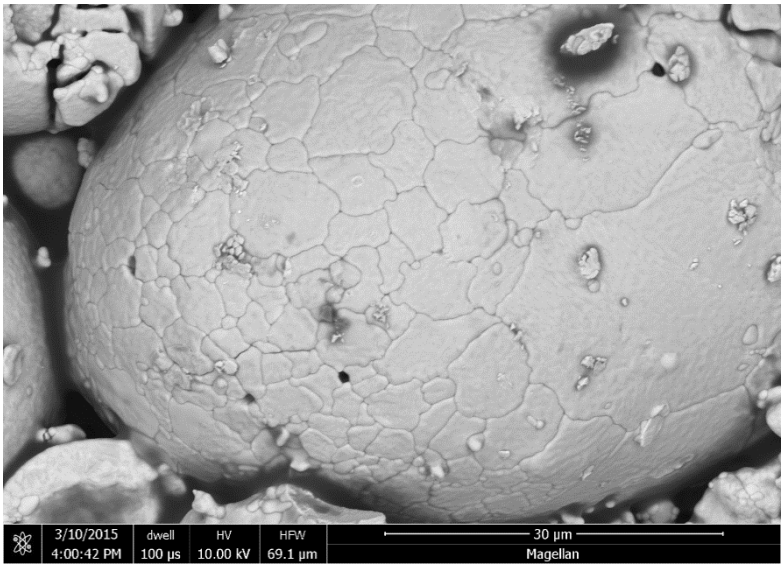

Fig. 12 An agglomerate of Zirconia present in the composite powder that has not been ball-milled before sintering

Uniaxial press

Powders are uniaxially pressed using the manual hydraulic press from SPECAC. The maximum load configuration for this compact bench top equipment is 15 ton. The dimensions of the pellets made were generally 13 mm in diameter and 8-10 mm thickness if the amount of powder is between 0.6-1 gm and the load applied is 5-6 ton. The Carver press is used to take out the pressed pellets from the 13 mm stainless steel die. Depending on the requirement 40 mm evacuable pellet die can be used. The powders must be tightly packed inside the die before pressing it hydraulically which will help increasing the density of the pressed pellets.

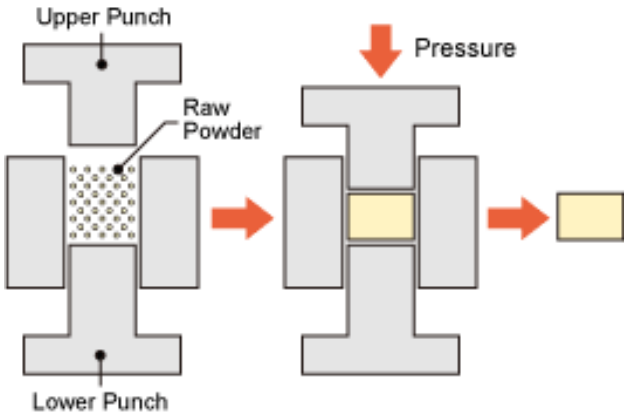

Fig. 13 Uniaxial Pressing
(http://global.kyocera.com/)

Cold isostatic press

Cold isostatic pressing (CIP) uses fluid to press the powders in a compact body. It is a process in which fluid creates pressure from all directions on a sealed rubber mold. Silicon rubber molds are used to put the powders in a cylindrical space and it needs to be packed densely before closing the lid. Sealed molds are put into balloons to make them airtight and then they are

drowned in the liquid inside the CIP. Silicon molds are made using Silicon rubber, heavy duty silicon lubricant and curing agent and it takes 24 hours to dry the molds. Once the molds are isostatically pressed up to 55 Kpsi for 5 minutes, the powders inside are pressed together in a compact cylinder which are called 'Green Bodies'. The dimension of isostatically pressed pellets are 6-8 mm in diameter and about 7 mm in length.

Sintering process

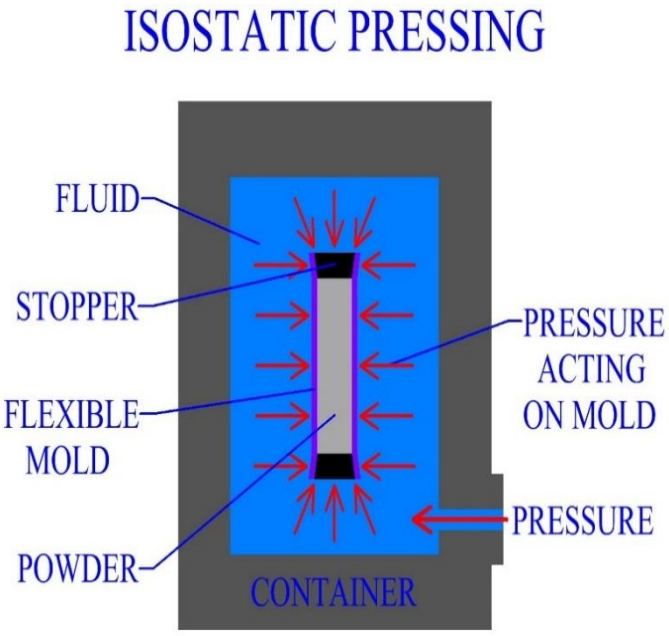

Fig. 14 Cold Isostatic pressing
(http://thelibraryofmanufacturing.com/)

The pressed pellets are then sintered using either box furnace or tube furnace depending on the atmosphere used during sintering. Dense YSZ pellets and porous YSZ pellets are sintered at very high temperature in presence of air. High purity alumina crucibles, boats and D-tubes are used to hold the pellets that sit on the powder bed and often covered with like powders. Sintering is a process where the atoms diffuse across the boundaries of particles, creating one solid pellet by

applying Pressure or temperature or both. The process reduces the porosity and enhances properties such as strength, thermal conductivity in metals or ceramics.

Full density can never be achieved by sintering materials; to maximize the useful properties of most ceramics, it is desirable to densify the sample as much as possible while keeping grain size to a minimum. This can require a compromise between density and grain size. In this project, most of the powders contain pore formers and soft weakening phase; resulting into porous fragile pellets where the average Zirconia grain size was about 1-5 microns.

Density measurement

For thermally sprayed ceramic abradable coatings, hardness and porosity are important properties to achieve an optimal performance for protecting the blade tip and causing minimal material transfer (7). Accurate density measurement was an important part of characterizing the physical properties of ceramic composites used in this project. The density of as-pressed pellets was calculated from the sample mass and volume. Mass was measured using a digital balance and sample volume was calculated from the external dimensions of the samples, which were right regular cylinders. There are several methods of measuring density including image analysis and electron probe microanalysis, but in this work Archimedes' method was used to determine the density of fired pellets (8). The bulk density of the sample was calculated from precise measurements of the dry, saturated, and suspended weight. Bulk density is the weight of an object divided by the bulk volume, V_b, the volume of solid plus all open and closed pores. According to the Archimedes' theorem, the bulk density of a solid is given by:

$$\rho_{bulk} = \frac{w_{dry} \sum \rho_{liq}}{w_{sat} - w_{susp}}$$

Where:

$\boldsymbol{\rho}_{bulk}$ is the bulk density of the sample

$\mathbf{w}_{dry}$ is the dry weight

$\boldsymbol{\rho}_{liq}$ is the density of the saturating/suspending liquid

$\mathbf{w}_{sat}$ is the saturated weight

$\mathbf{w}_{susp}$ is the suspended weight

The volume of open and closed pores can also be calculated using Archimedes' measurements. The volume of open pores, V_o, is given by:

$$V_o = \frac{w_{sat} - w_{dry}}{\rho_{liq}}$$

The volume of closed pores can be calculated only if the theoretical density of the material is known. The dry weight divided by the theoretical density gives the true volume, V_t. True volume is the volume of solid in the pellet. The volume of closed pores, V_{cp}, and volume of bulk sample, V_b is then:

$$V_{cp} = V_b - V_o - V_t$$

$$V_b = (w_{sat} - w_{susp})/\rho_{liq}.$$

It has been observed that for different powders the densities are different. The final density of a sintered pellet depends on sintering time and temperature.

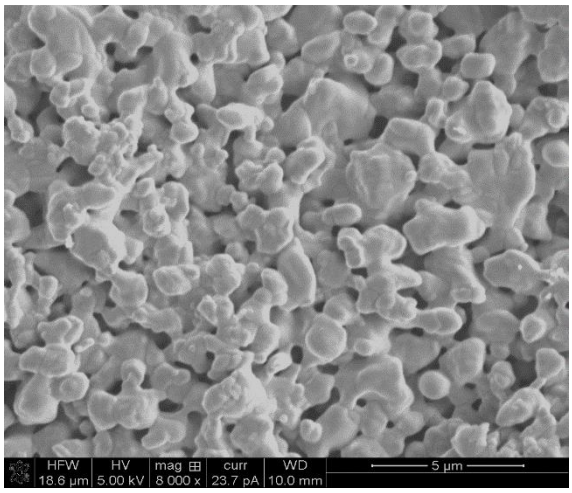

Fig. 15 Porous pellet

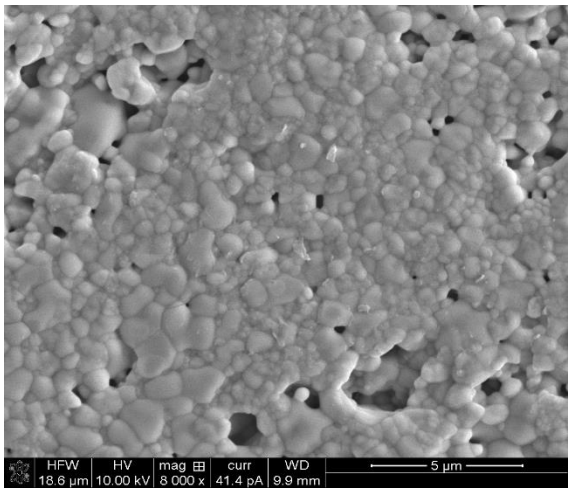

Fig. 16 Dense pellet

Hardness test

Hardness is not an intrinsic property of materials; it refers to the resistance of a material to bending, abrasion or cutting. Hardness could be measured using different methods such as Rockwell hardness test, Vickers hardness test, Brinell hardness test, Knoop hardness test etc. The Vickers hardness test will be discussed in the following section since it was used to measure the hardness of the composite materials.

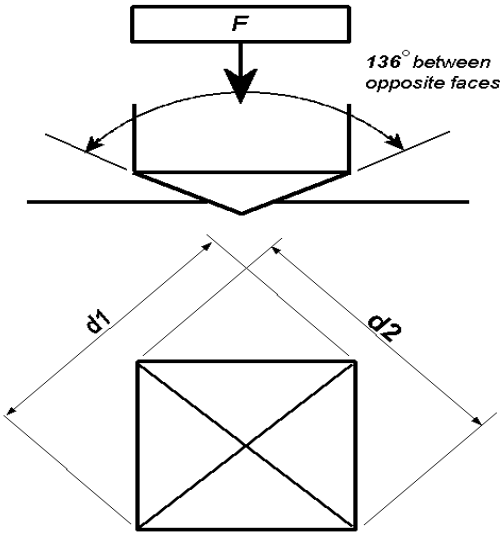

Fig. 17 Vickers Hardness Test Schematic
(http://www.gordonengland.co.uk/)

In Vickers hardness test method (Fig. 17) the test material is indented with a diamond indenter. The tip of the indenter is a right pyramid with a square base and an angle of 136 degrees between opposite faces. Load is normally applied to the surface of the sample for 10 to 15 seconds to measure hardness. The two diagonals of the impression left on the surface after removal of the

$$HV = \frac{2F\sin\frac{136^o}{2}}{d^2} \qquad HV = 1.854\frac{F}{d^2} \text{ approximately}$$

load are measured using a microscope and their average calculated.

Where,

F= Load in kgf

d = Arithmetic mean of the two diagonals, d1 and d2in mm

HV = Vickers hardness

In this project, a 9 Kg-f load was used and the diagonals were measured using the micrometer attached to the hardness test microscope for denser pellets, and electron microscopy technique for softer materials.

Yttria stabilized Zirconia is well known for its high hardness and flexural strength; it has better mechanical strength and fracture toughness than Alumina. Sometimes, Dysprosia (Dy_2O_3) is used as dopants replacing Yttria as it has been studied that they decrease the thermal conductivity and improve thermal shock behavior of Zirconia (9). The well sintered YSZ pellets could reach 99% density and the hardness is about 12.2 GPa.

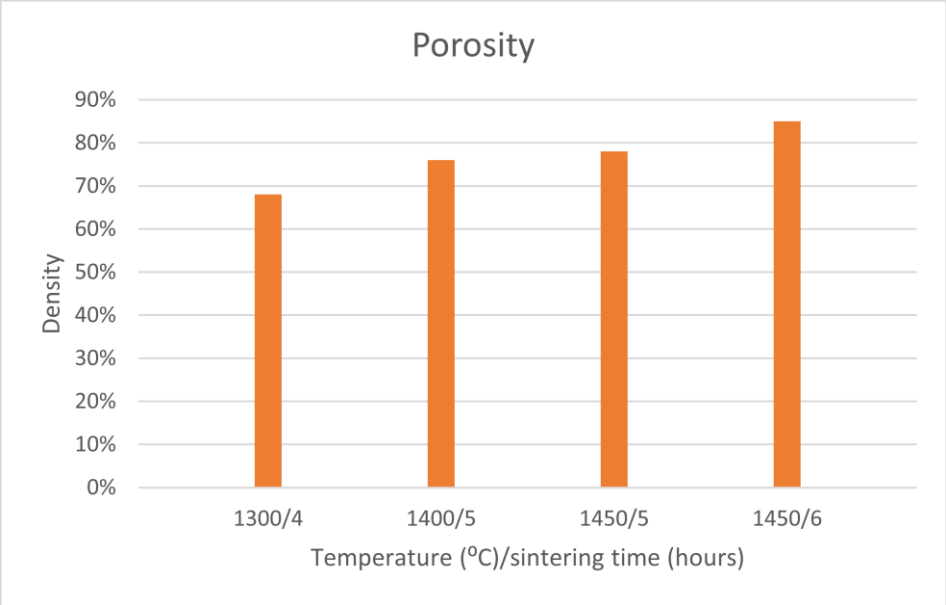

Fig. 18 Porosity decreases with sintering time and temperature

It is possible to use the same powder to make pellets of varied density by changing the sintering time and temperature or by adding extra polyester to the powders. The purpose of making pellets of different density was to study the effect of porosity on composite materials hardness.

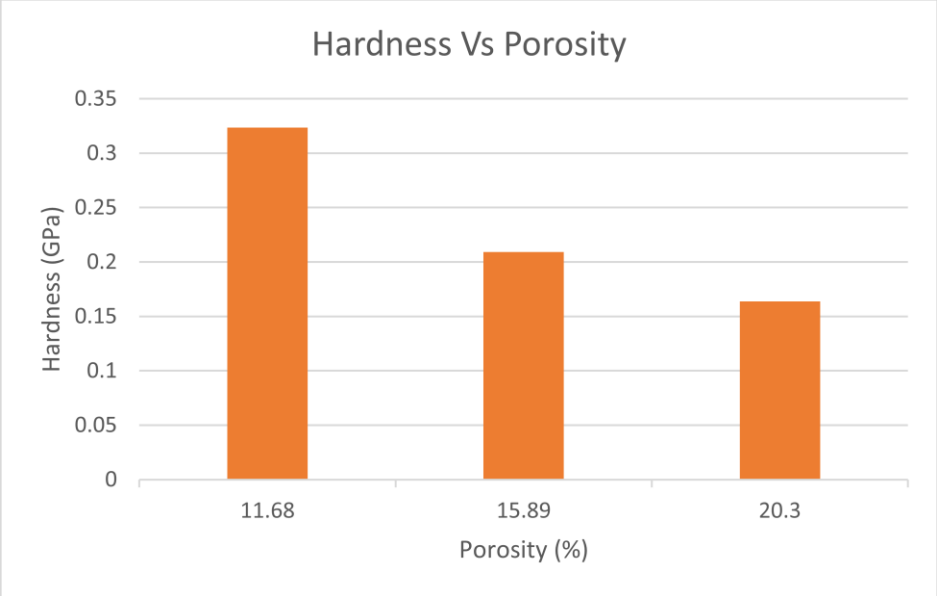

Fig. 19 Hardness decreases with increasing amount of porosity

Metallography techniques

After sintering the composite powders into dense, rigid pellets, a high-speed diamond blade saw was used to section them into desired shape and sizes. The pellets were first glued to a square metal plate using crystal bond, then the plate was attached to the stage of the high speed saw. This stage can be moved manually in two directions and the motion in the third axis is automatically operated; distance in mm has to be measured and entered digitally in the machine before starting single cut/ multiple cut.

After the pellets were cut, they were mounted and polished using grinding and polishing paper, suspension or lapping films. A polishing jig is used to make sure that the polished surface is flat, otherwise focal plane needs to be adjusted every time position changes during imaging. Starting from the SiC grinding paper #120 the polishing procedure generally goes up to #2400 grits and

then Buehler mini-met polishers are used to fine polish the pellet with 3, 1 and 0.25 micron diamond polishing suspension. If the pellets are much smaller than the polishing plate mini-mets are not effective, and diamond lapping films are then used. There are mainly two types of diamond lapping films available for ceramic materials based on the back support: Plain or Pressure sensitive adhesive, and the available abrasive sizes ranges from 30 micron to 0.1 micron. It is always recommended to use optical microscopy after each polishing step to keep track of the polishing quality before taking the finished surface for imaging.

Softer and/or porous materials could be damaged during the cutting, grinding and polishing procedures. Therefore, they must be molded in epoxy using resin, hardener and curing agent, dried in vacuum and then cut into manageable shape before starting metallography processes. In this way, samples are better protected and safer handling can be achieved. It is important to follow the procedures of cutting, mounting and polishing carefully to minimize the loss of material and inclusion of impurity in the sample.

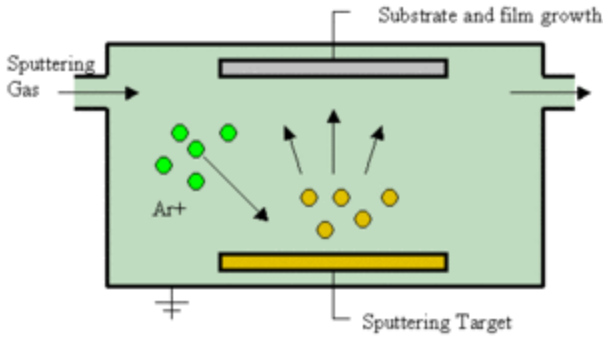

Fig. 20 Sputter coating technique illustrated

(https://en.wikipedia.org/wiki/Sputter_deposition)

Samples are then mounted on the available stubs used for microscopy analysis and sputter coated with iridium to make sure the sample is not charging when hit by electron beam in high voltage/high vacuum SEM mode. Typically a metal, such as Iridium, Carbon, gold/palladium alloy is used, metal coatings are also useful for increasing signal to noise ratio as the heavy metals are good secondary electron emitters.

IMAGE ANALYSIS TECHNIQUES

There are several instruments that have been used for the purpose of image analysis for this project. After the metallography processes were done, surfaces were checked using optical microscopy to confirm that the samples are well-polished and flat. Then the topological features were studied in high resolution scanned electron microscopy. Back-scattered electrons help in detecting the underlying surface chemistry and the energy dispersive spectrum verifies the chemical composition in the sample. This chapter describes each technique in more detail.

Optical microscopy

The optical microscope uses visible light and an arrangement of lenses to create magnified image of a small sample. The objective lens is typically the highest powered lens with a very short focal length. The object, when focused using the lens system, is enlarged and inverted.

In present days optical microscopes are rarely used for image analysis of small samples since the magnification only goes up to 1000-2000 times. This is a physical limit imposed by the wavelength of the light. Whereas, electron microscopy has a much higher resolution and it can magnify objects down to nano scale. They also possess a greater depth of field than light microscopy.

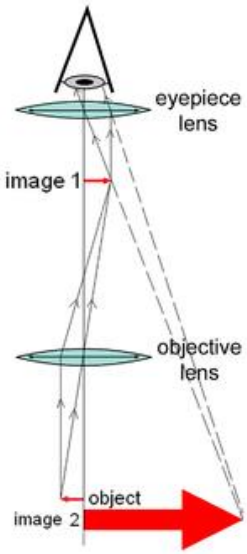

Fig. 21 Optical Microscopy principle
(http://figures.boundless.com/)

Scanned electron microscopy (SEM)

SEM uses a highly concentrated electron beam instead of a beam of light, which is produced by the electron gun located at the top of the system. Two types of electron guns are used by SEMs; Thermionic guns that heat a filament until electrons stream away and Field emission guns that generate a strong electrical field to trigger the electron beam.

The chamber of SEM is always under high vacuum; electron beam enters the chamber and is directed toward the specimen by the lens system in order to maximize efficiency. The main function of maintaining vacuum inside the chamber is to remove the risk of small particles that could obstruct the electron beam and deflect the electrons coming from the specimen, obscuring the results.

When a specimen is hit with an incident beam, it emits X-rays and three kinds of electrons: primary backscattered electrons, secondary electrons and Auger electrons. The SEM makes use of backscattered electrons and secondary electrons. An electron detector (usually Evarhart-Thornley detector, which is a type of scintillator-photomultiplier system) picks up the rebounding electrons and converts them into digital information which is then translated onto a screen. Secondary electron signal provides topographical information in a consistent and coherent manner.

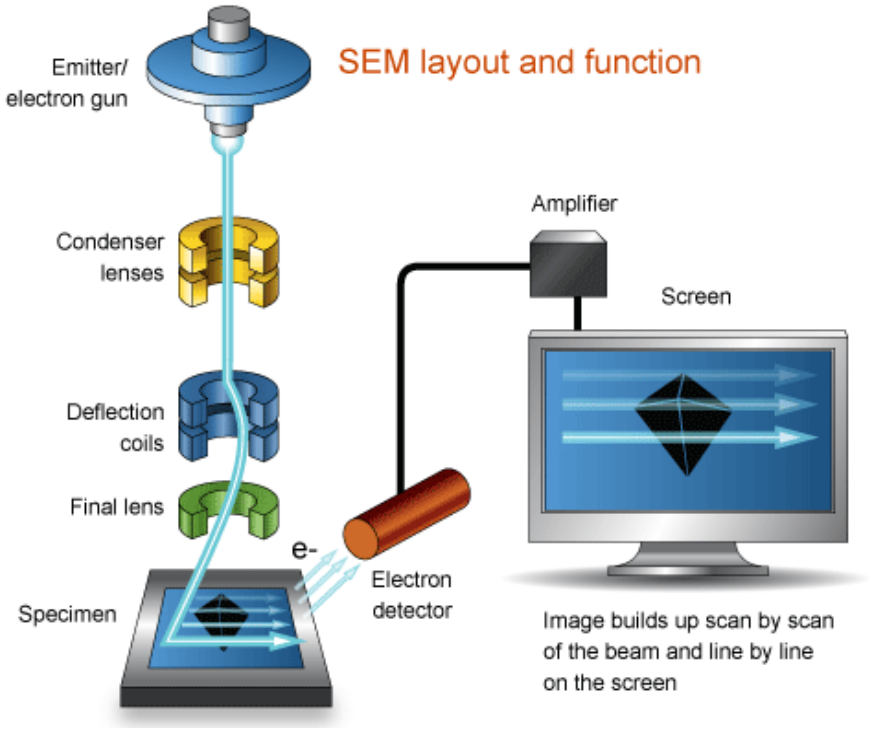

Fig. 22 Illustration of SEM stages
(http://bioaccent.org/microbiology/)

Back-scattered electron microscopy (BSE)

BSE detector detects the electrons scattered back from the sample. Interaction between the electron beam and the specimen produces a variety of elastic and inelastic collisions inside the sample. Elastic scattering changes the path of the incoming beam electrons without changing their kinetic energy. These high energy electrons come out of the sample and are then detected by the BSE detector.

The atoms with higher atomic number have greater possibility of interacting with the high energetic electron and deflect its way since they possess larger surface area. Thus, a brighter BSE intensity represents materials with higher atomic number (Z) in the sample, and dark areas have lower Z. BSE images are very helpful for obtaining high-resolution compositional maps of a sample and for distinguishing different phases.

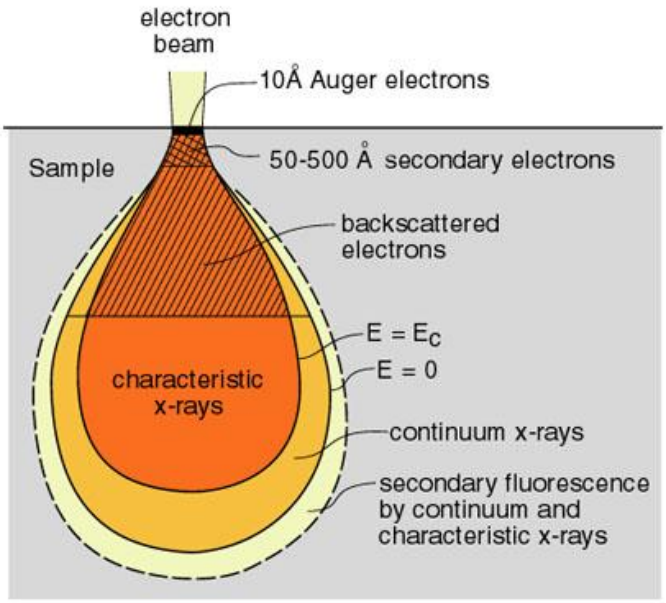

Fig. 23 Backscattered electron schematic

(http://nau.edu/)

Energy-dispersive X-ray spectrometry (EDS)

EDS is used in conjunction with BSE detector and multichannel analyzer. Incident X-ray photons cause ionization in the detector, producing an electrical charge, which gets amplified by a preamplifier. A silicon lithium detectors Si (Li) or Silicon drift detectors (SDD) are commonly in use for their better energy resolution. The energy spectrum is displayed in digitized form with the x-axis representing X-ray energy and the y-axis representing the number of counts per channel. Both detector and preamplifier are cooled with liquid nitrogen which helps reducing the electronic noise. EDS is used for elemental analysis and chemical characterization of the sample.

Here some SEM, BSE images with EDS spectra will be discussed that provide important information regarding the surface, composition, chemistry of sintered pellets and their distribution. Since the matrix is Yttria/Dysprosia stabilized Zirconia for each powder, it is important to know some of the properties that explain the images.

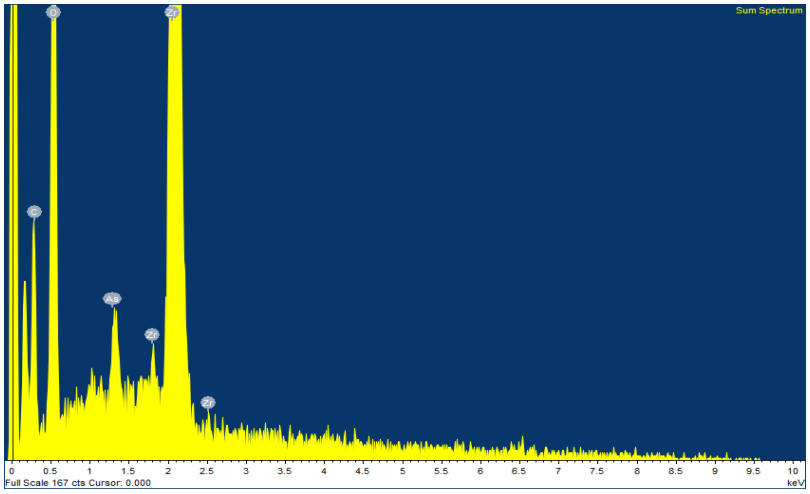

Fig. 24 EDS spectrum of abradable composite powder

Zirconia is a ceramic oxide comprised of two elements: Zirconium (atomic number 40) and oxygen (atomic number 8). With Oxygen, Zirconium forms a colorless solid oxide that has exceptional fracture toughness and chemical resistance, especially in its cubic form. Since Yttrium (Y), Dysprosium (Dy) and Zirconium (Zr) are the heaviest in the abradable system, they will also be the brightest when imaged using BSE.

Boron present in the Boron Nitride compound, on the other hand, is the lightest element of the system (atomic number 5) and will be the darkest sites in the image. Hexagonal Boron Nitride is expected to be the lubricant phase in the system that will hold the YSZ grain together forming a network that will enhance the machinability of the seal keeping other useful properties same. .

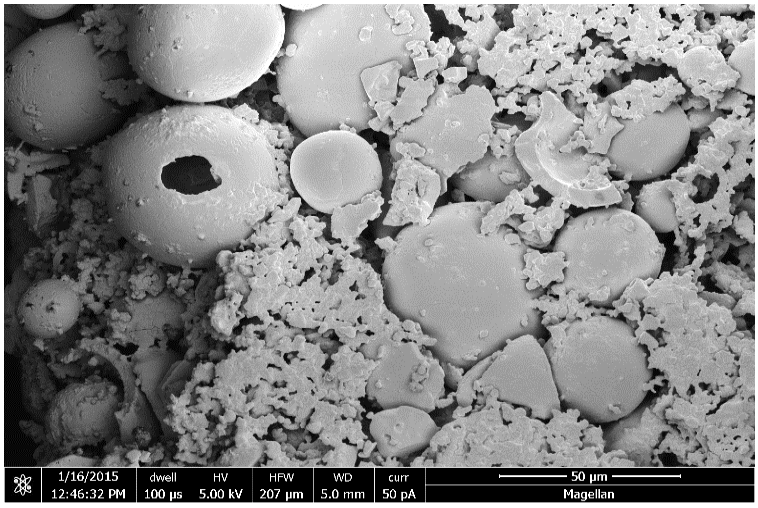

Fig. 25 Abradable composite: DySZ, h-BN and Polyester. SEM images are intuitive; it is clear from this image that the surface of the pellet is uneven, the agglomerates did not break evenly and it is not very well sintered

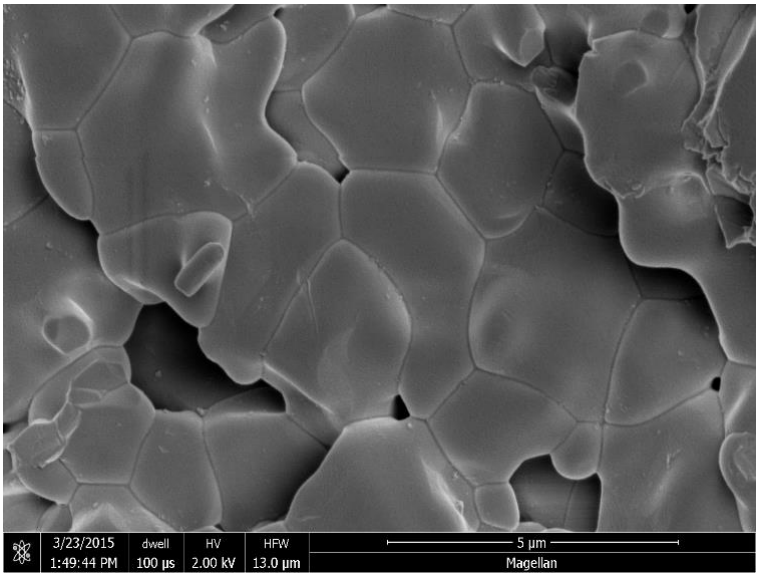

Fig. 26 SEM images also contain information about the grain growth of material. Here is the 8YSZ sintered at about 1400 ^{0}C for 2 hours

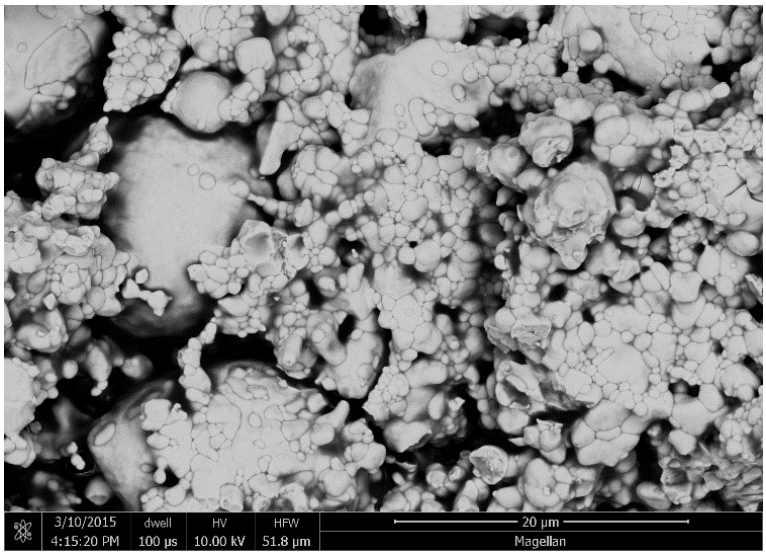

Fig. 27 BSE image of one of the abradable composite that has a network of h-BN phase interconnecting the grains of the DySZ powder. It also contains a lot of pores throughout the pellet. The brightest grains are Zirconia and the grey phase represents

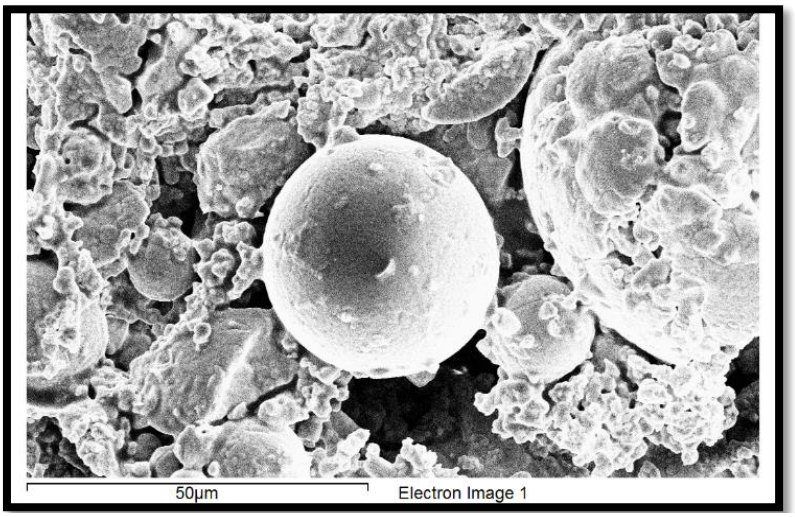

Fig. 28 Energy Dispersive Spectrometer to quantify the relative amounts of elements present. Result: Zr and O were dominating whereas the amount of Yttrium (Y) and Boron were negligible

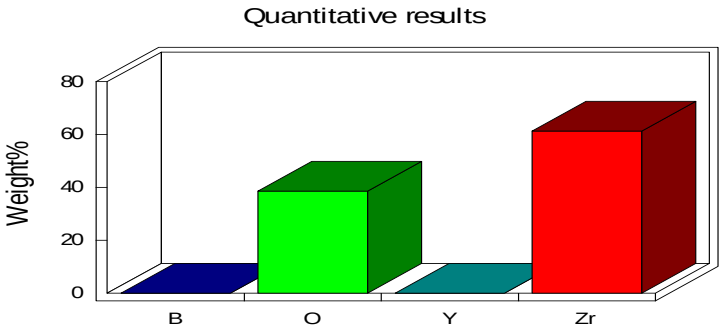

Fig. 29 Weight percentages of detected elements

Troubleshooting

Analyzing Boron (atomic number= 5) using EDS was always very hard; problem for detecting light elements are the low fluorescence yield, absorption and overlapping peaks. Even though the excitation volume of light elements is generally larger than for heavier elements when hit by incoming beam with same accelerating voltage, less X-rays are produced because the formation of Auger electrons is favored. Due to the low energies of these electrons, many of the X-rays produced get absorbed before they can reach the sample surface. Moreover, some of the photons that come out of the sample and directed towards the detector might get absorbed by the detector entrance window (Beryllium) and other components of the detector. Therefore without a window less SEM detector it is hard to confirm the presence of Boron.

The abradable powders containing hBN were very fragile even after sintering; the pellets were tested and found that a dense YSZ pellet is 20 times harder than the composite pellets. Although it was an expected behavior from the abradability point of view, it was difficult to handle the pellets during density tests and hardness tests. The reason behind is that the weakening BN phase surrounds the zirconia particles making the bonding between YSZ particles fragile. The porous structure also makes it softer as previously discussed. The problem will be naturally solved when the powders are sprayed thermally on a harder bond coat/ substrate.

Hexagonal Boron Nitride is used in the YSZ composites as the release agent. The only drawback with this compound is when sintering the composite in oxidizing atmosphere (Box furnace) at temperatures higher than 1000℃, hBN reacts with Oxygen (since it is not stable in presence of O_2 and volatilizes in humid environment at very high temperatures) (10) .

Boron reacts with the oxygen to form Boria (B_2O_3) and then boro silicate glass, if silica is present in the environment (even if in a very small amount), both of which could form a glassy phase along the grains of the matrix. This glass phase is the region where coating failures will take place since it is an amorphous phase and is not capable of absorbing the impact energy created during interaction.

Volatilization will be initiated after oxidation of BN to B2O3 and the subsequent reaction with water to form highly stable HxByOz gaseous products. As a result the composite will have added pores to its microstructure and unevenly distributed h-BN in the coatings likely include the scattered presence of B2O3.

$B_2O_3 + H_2O = 2\ HBO_2\ (g)$

$2\ B_2O_3 + 6\ H_2O = 4\ H_2BO_2\ (g) + O_2$

$B_2O_3 + 3\ H_2O = 2\ H_3BO_3\ (g)$

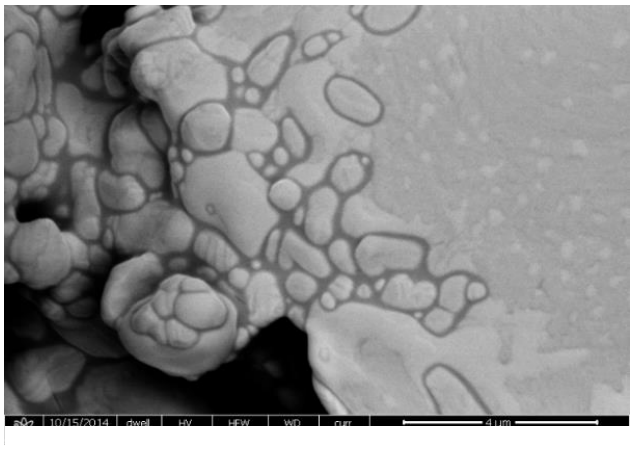

Fig. 30 BN containing composite pellet sintered at high temperature in presence of Oxygen

EXPERIMENTS AND RESULTS

In this section experiments executed to investigate the effect of humid environment on these abradable samples has been discussed beginning with the water vapor exposure test set up, conditions and experiment results. Then the thermal conductivity test and the mechanical tests have been described and their relevance regarding the current system has been explained.

Sintering BN powders in tube furnace

In order to prevent oxidizing BN, a tube furnace with an inert atmosphere was used to sinter the BN-containing abradable powders. An Alumina tube was used for the test and only Argon (Ar) was flown at 80 sccm throughout the tube. Since the BN is stable up to temperatures of 2800 ℃ in inert atmospheres, it was safe to sinter the powders at about 1400℃. Four abradable pellets were sintered in two batches at different sintering temperature and time using a dee tube and a plate. The accessories used were strictly made of very high purity Alumina. Before starting the sintering process, a bubble test was performed while flowing gas through the tube to ensure that the complex set-up does not have any leakage. The gas out from the exhaust side goes through a glass tube partially filled with DI water forming bubbles confirming the gas flow; it is important to measure the flowrate of bubbles during the experiment to ensure the constant flow.

The first batch of samples were sintered in inert atmosphere at 1349℃ for 9 hours and the sintering time for the second set of two CIP samples were 1400℃ for 5 hr in Ar environment. The duration of these experiments was about 15 hours, starting from the ramp up (ramp rates were 5℃/min) until the temperature went down to essentially room temperature, but it varies

with the dwell time at sintering temperature and pre-sintering heating time if required. The resulting pellets were well sintered, fit for Archimedes test and hardness test.

Dry run: 1335^{0}C for 5 hrs (N_2:O_2= 80:20), 80 sccm flowrate

Weight and dimensions of the sintered composite powders were measured, then cut in halves, polished carefully to minimize the loss of materials, and prepared for the controlled environment test. First, in the dry test halves of four different samples were exposed at 1335℃ for 5 hr, N_2 and O_2 were flown through the alumina tube in the ratio of 80:20 at 80 sccm (standard cubic centimeter per minute) flowrate. After the exposure the pellets were very fragile, thus handled carefully and taken to the sputter coater to make them ready for SEM. As the interest was to study the microstructure and the degradation of the surface, the pellets were not polished before coating with a conductive metal layer (approximately 5-10 nm).

Wet run: 1335^{0}C for 5 hrs (N_2:O_2= 80:20), 80 sccm flowrate with 30% water vapor

For the wet run all of the procedures were done as before, after that the other halves of those four samples were exposed in the controlled environment. The ratio of N_2 and O_2 was kept same as before but the flowrates were reduced and 30 vol% water vapor was introduced in the inlet stream. The total flowrate was also kept the same to confirm that any changes in the microstructure of the pellets were due to water vapor and nothing else.

Water vapor exposure test and results

Now that it had been established that the composite powders do contain enough porosity and are significantly softer compared to pure YSZ materials, it could be said that these are initial promising features as abradable seals. The next step is to determine their potential in an IGCC plant environment; which leads this project to set-up a controlled environment tube furnace test using a water tank to supply the water vapor. At the end of the experiment pellets were taken to sputter coat with Iridium and were ready for SEM.

Weight loss

After the dry run and wet run samples were weighed to see if there is any loss/gain of materials involved. Dry run samples showed 3-6% weight loss and wet run samples have shown 6-7% weight loss after exposure. BN (density 2.3 g/cc) reacts with water to form Boron tri oxide (B_2O_3, density 2.460 g/cc) at temperatures above 1000^0C, indicating loss of weight after exposure in air. But the amount of BN present in the system is negligible (0.8-1 wt%), hence the loss would be minimal. Furthermore, amount of polyesters (density 1.37 g/cc) is higher in comparison to BN which burns out during the heat treatment above 500^0C. Hence the loss of weight. In the wet run, B_2O_3 reacts with water vapor and volatilizes; hence higher weight loss is observed after wet exposure.

Surface evolution

The effects of water vapor on high temperature oxidation have always been of scientific interest. The presence of water vapor is known to increase the oxidation rate which impacts the oxide structure, stability and decreases the lifetime. Hence the knowledge of what is happening when the samples are exposed in the humid environment is immensely helpful before proceeding with thermo-mechanical tests. The surfaces of the wet run samples were noticed to develop cracking; it is a common occurrence in ceramic oxides exposed in humid atmosphere at high temperature. This process is similar to how mud cracks appear after rain when the wet mud dries off. Water vapor enhances the oxidation rate and grain growth in the material, it also volatilizes the weakening phase strengthening the bonding between YSZ particles. Afterwards, when the temperature drops, the grains shrink, pulling away materials from neighboring particles leading to crack growth.

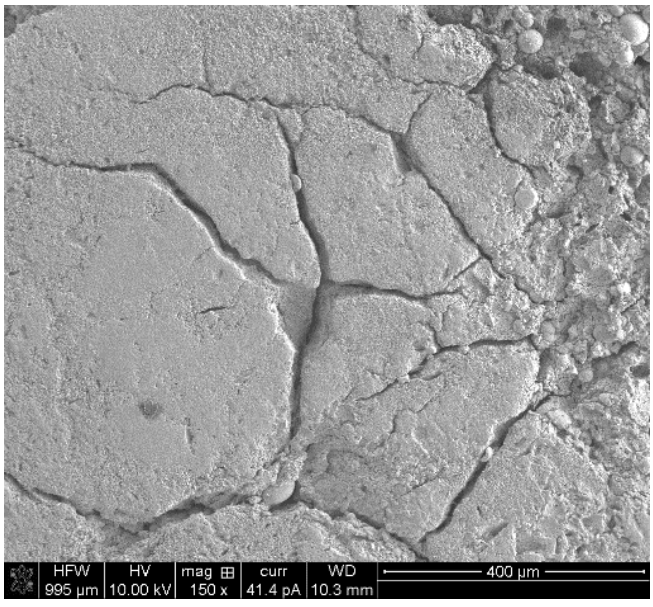

Fig. 31 Crack growth on the surface of wet run sample

The other noticeable feature in the wet run sample is that the blisters are unevenly distributed on the surface. One possible reason for this phenomenon is that the hydrogen in the gas stream is reacting with the dissolved oxygen to form water bubbles inside the composite subsequently nucleating pores and swelling the surface. Since the coating contains BN which volatilizes in humid environment, there is a high probability that some amount of Boron oxi-hydrides (gas phase) are also getting trapped inside the composite.

Here, the system of interest involves a porous two phase ceramic composite material and the response to the humid environment was expected to be equally complicated. Mainly as the system contains Boron Nitride; it volatilizes in humid atmosphere leaving void spaces that are different from pores created by burning out the polyesters. That indicates more voids in the system that should not degrade the mechanical performance.

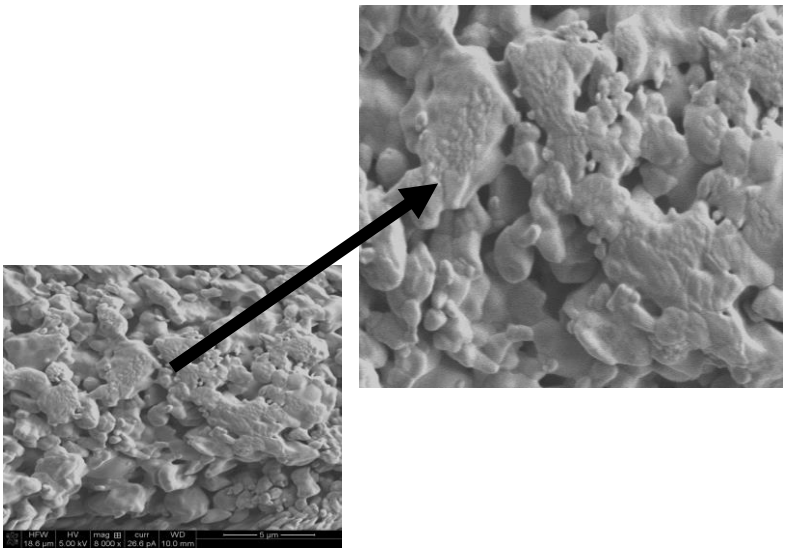

Fig. 32 Swelling on the surface

But in reality, more porous structure have been observed in the dry air exposure sample, the surface of the wet run samples looks smoother and less porous. Boron could not be analyzed using BSE or EDS in any of the samples. Further work is needed to understand if the change apparent on the surface remains there or goes deeper into the material resulting into bulk diffusion (11). To verify if the abradable properties deteriorate with presence of water vapor or if the moisture aids the properties, thermal conductivity test and mechanical performance tests are required.

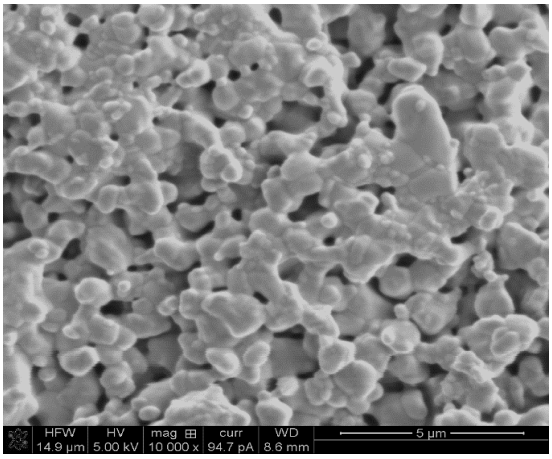

Fig. 33 Dry run sample

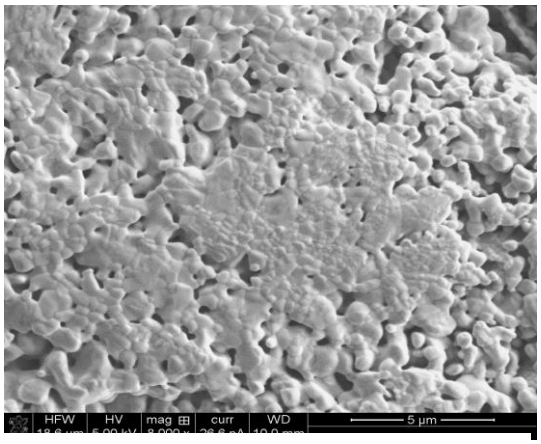

Fig. 34 Wet run sample

Thermal conductivity test

Another method to investigate the feasibility of porous YSZ-hBN system in IGCC environment is studying the effect of humid environment in the thermal properties of these composites. Yttria stabilized Zirconia has a very low thermal conductivity which is one of the main reason of using it for the high temperature applications. Fully dense, large grain size YSZ with 6–8 wt.% Y2O3 stabilization has a reported thermal conductivity in the range 2.2–2.9 W/(m K). On the other hand, range of thermal conductivity of hBN is 30-600 W/mK depending on the nature of their crystal plane.

Thermally sprayed ceramic abradable composite made out of these materials possess a low Thermal Conductivity and are chosen coating material for hot section of turbine, but as the Boron Nitride destabilizes in humid environment the thermal conductance must decrease. Theoretically, lower thermal conductivity means smaller thermal gradient and more stability at high temperature, which is desirable for high temperature applications. Therefore it is important to investigate the change in thermal conductivity of these materials when exposed in water vapor environment. A steady state bi-substrate test set up has been developed based on the paper ‘A steady-state Bi-substrate technique for measurement of the thermal conductivity of ceramic coatings’ by J. C. Tan et al. solely for this purpose which would predict the applicability of abradable coating in IGCC environment (12). With this method, only the temperature drops across the sample and the heat flux are required to obtain the thermal conductivity. This is a well-established approach for bulk material, although there is always a concern about lateral heat losses and maintenance of unidirectional heat flow conditions.

Table 2 Thermal Conductivity chart for 303 Stainless Steel

Temp (K)	Thermal Conductivity (W/mK)
293	14.76
350	15.79
400	16.61
500	18.28
600	19.77

Fig. 23 shows a schematic of the setup. The sample, in this case a disc of 13 mm diameter, is sandwiched between two metallic substrates. These substrates act as flux meters, four K-type thermocouples (T_1 to T_8) are inserted into holes at known distances, drilled to the centerline of each block. A minimum of two temperature readings are required from each substrate to determine the heat flux, but additional values allow it to be more accurate and also validates the

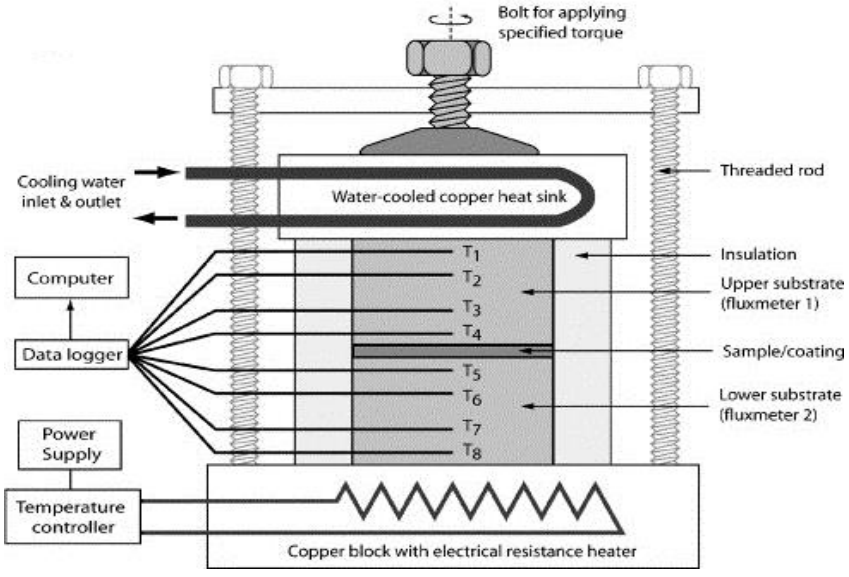

Fig. 35 Bi-substrate Uni-axial Thermal Conductivity set up (12)

assumption of uni-directional heat flow. Since the thermal conductivity of 303 stainless steel is well known over a wide temperature range (Table 1), it can be used in measuring the heat flux across as the chosen metal substrates. The blocks are insulated laterally with a suitable ceramic fiber blanket material.

Temperature gradients are generated by heating the lower substrate with a cartridge heater, while heat is continuously removed from the upper substrate via a water-cooled copper heat sink. In order to maintain constant rates of heat injection and removal, the heater power and cooling water flow rate are fixed and the system is left for a suitable time to equilibrate, with the thermocouple outputs being recorded. The validity of the assumption of unidirectional heat flow is checked by comparing the average heat fluxes through the two substrates. In general, it is possible to ensure that these fluxes are within 5% of each other and this is considered to represent a sufficiently accurate approximation to uni-directionality.

The heat flux per unit area could be calculated (assuming unidirectional flow without any heat loss) using the Fourier's law in one-dimensional form:

$$q_x = -k\frac{dT}{dx}$$

Where, q_x= Local heat flux density (W/m^2) = Q/A

K= Thermal conductivity of the material (W/mK)

(dT/dx)= Temperature gradient (K/m) = $\Delta T/L$

The purpose of using this formula is to compare the heat flux between the reference and the sample as the heat flow throughout the system will remain the same for both the substrate and

the sample. From that, thermal conductivity of the sample can be calculated when the temperature across the sample is known. The mean heat flux can be written as:

$Q = (Q_{upper}+Q_{lower})/2$

Q_{upper} = Heat flux through the upper substrate

Q_{lower} = Heat flux through the lower substrate

The conditions are presumed to approximate to one-dimensional heat flow when:

$(Q_{upper} - Q_{lower})/ Q \leq 10\%$

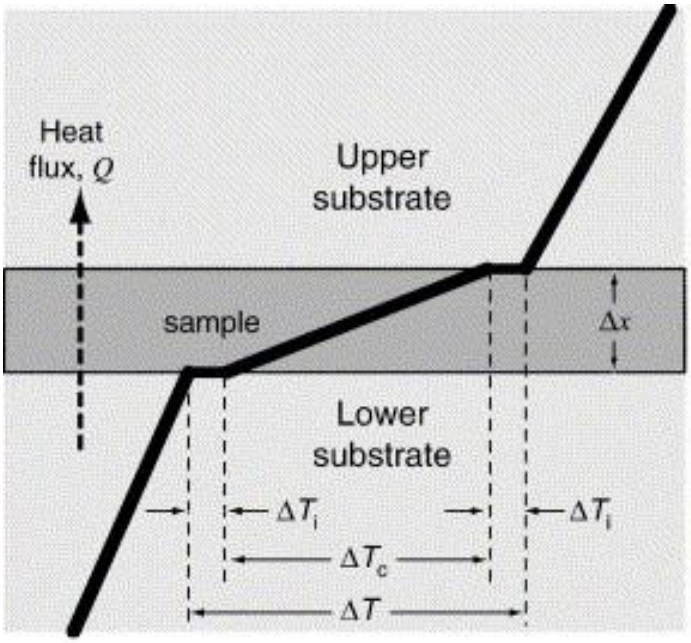

Fig. 36 Temperature drops across substrates, sample (coating) and two interfaces (12)

Fig. 36 shows a schematic of the temperature profile under steady-state conditions established across the substrates, sample and two interfaces which were used to improve conduction between the sample and the substrates. Assuming no lateral heat losses, the same flux flows through substrate, coating and interfaces, so that:

$Q/A = K_s*(\Delta T/L_s)$

$Q/A = h_i*(\Delta Ti/L_i)$

$Q/A = K_c*(\Delta Tc/L_c)$

h_i= Thermal conductance of the interface

[*s, c and r represents substrate, coating and interfaces]

The total temperature drop, ΔT is composed of drops across the coating and across the interfaces:

$\Delta T = \Delta T_c + 2*\Delta T_i$

*[ΔT_i multiplied by 2 because there are 2 interfaces]

By substitution and rearrangement of these equations,

$$\frac{\Delta T}{Q} = \frac{\Delta x}{Kc} + \frac{m}{h}$$

Plotting $\Delta T/Q$ versus Δx, the slope and intercept are given by $1/K_c$ and m/h, respectively. Both K_c and h can thus be determined from such a plot by using same sample with different thicknesses. In this project, a silicon thermal pad with 5 W/mK thermal conductivity is being used. Since the value of 'h' is already known, the equation below can be used to compare the heat flux or to calculate the thermal conductivity of the sample.

$$\frac{Q}{A} = \frac{Ks}{Ls} * \frac{\Delta T_u + \Delta T_l}{2} = \frac{Kc}{Lc} * \Delta T$$

ΔT_u= Temperature difference in the upper substrate

ΔT_l= Temperature difference in the lower substrate

Presently the set-up is being calibrated for different temperature ranges using three different thicknesses. A dense YSZ pellet will be tested for the reference thermal conductivity, then

porous YSZ and porous YSZ containing BN will be measured. Final goal is to compare the heat flux through the dry run and wet run pellet that would help to understand the evolution of thermal properties of composite materials in humid environment. This method is simple but precise, it can be applied to ceramic coatings of different thickness and porosity levels.

Laboratory developed Mechanical test: BARB test

The ceramic abradable coatings are by nature brittle, by structure porous and fragile. They must not be very hard to damage the blade tip, too much softness will dictate erosion. They are composites made of very hard materials that has voids in them and a network connection of releasing agent throughout its matrix. The complexity in the physical structure of these coatings calls for refined mechanical testing to predict the coating failure and study the degradation mechanism. Coating durability is dependent on the interaction between the crack driving forces and the resistance to crack propagation through the coating or interfaces between the coating and the substrate. The BARB test is a mechanical test technique that has been developed by Kagawa et al. few years ago to facilitate evaluation of the fracture characteristics of coatings and interfaces in thermal barrier coating (TBC) systems (13) (14). This project would use the same set-up to study the crack propagation through the abradable coating materials and to predict the applicability of those in high temperature humid combustion environment.

The test set up is designed to provide flat surfaces that transmit force to the cut edge of the ceramic composite layer during relative change of the substrate. It is a primary concern for this test to ensure proper contact of the coating with the test fixture, since the coatings are thick

enough (≤1 mm), this should not be a problem. Here, Sapphire plates were used as load transfer or support blocks.

The BARB test would have the capability of gauging the strain, producing the data of load vs displacement curve and above all a digital camera is attached to this setup which would capture the crack propagation in real-time. The exposed (dry and wet environment) samples would

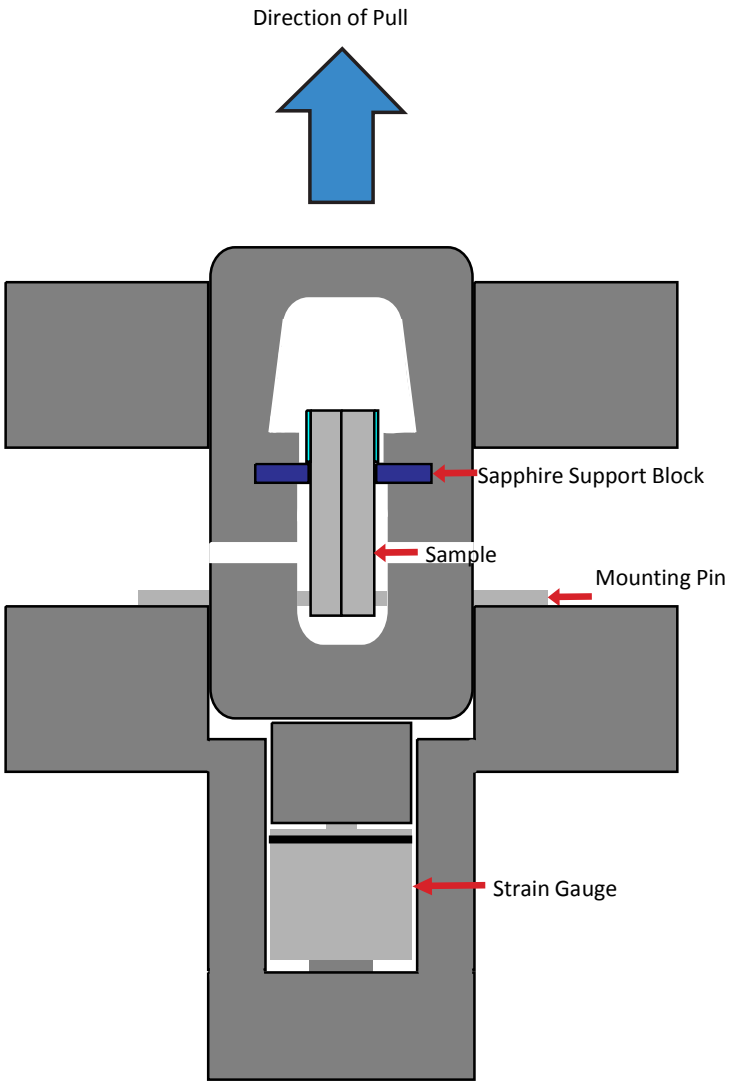

Fig. 37 A schematic of the barb test loading fixture is shown in here, illustrating the overall technique

contain different amount of stress across the coating and substrate layers due to the thermal cycling process that would leave the outer layers in tension. Overall, it is important to study the crack growth and coating failure of the as-sprayed composites, after dry exposure and after exposing in humid combustion conditions.

FUTURE GOALS

The objective of this chapter is to demonstrate other relevant tests and experiments that could be done to make further progress in this investigation. Few exposure tests controlling different parameters, a standard test to directly quantify abradability property and two potential abradable coatings for IGCC environments will be discussed.

For the further study of the microstructure few more experiments are required to be performed to achieve a concrete conclusion. The comparative study between dry run and wet run is based on the short time exposure of the abradables which is not sufficient; longer time exposures would contribute more evidence in support of the anticipated mechanism. Increasing the gas flowrate and amount of water vapor to 45% (harsher environment) could be another way to see if the surface degrades in a faster rate or remains constant keeping the exposure time same. It is also advisable to examine the association between reactivity of Boron Nitride and the change in surface chemistry.

Abradability rig test

A laboratory scale rig is being designed based on a standard mechanical test to investigate the abradability properties of the composites at high temperature. The test rig consists of a rotating test blade (tipped or un-tipped) and a stationary test shroud segment coated with the abradable system (15). Evaluation of the rub mechanism and generation of wear maps will be very informative using this set up. The test will incorporate flame generator to simulate the high

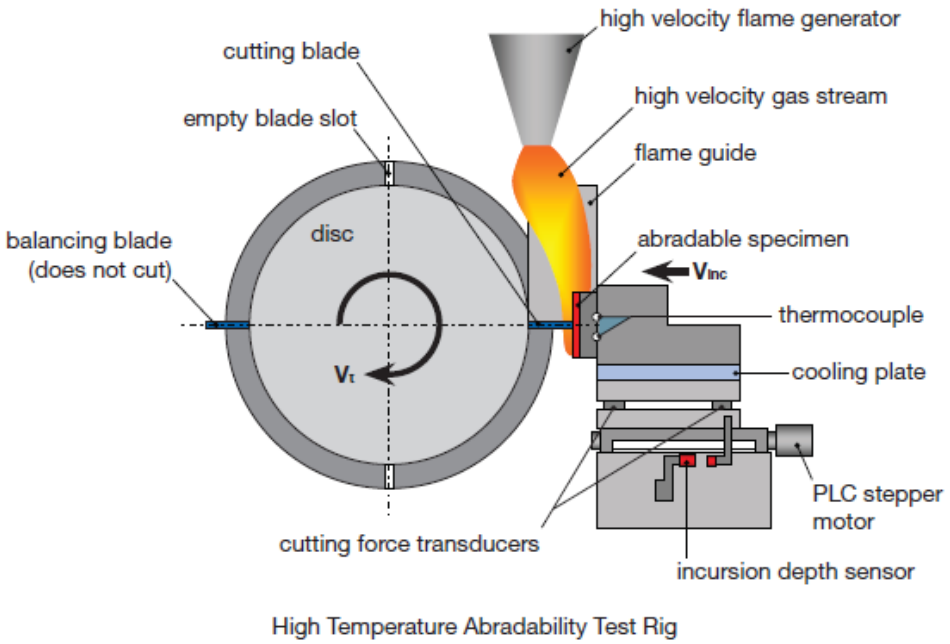

Fig. 38 Oerlikon abradable incursion test facility based in Winterthur, Switzerland (15)

temperature effect and cooling plate at the other end of the specimen to develop thermal gradient across the sample. This technique portrays the stress distribution in the actual turbine stages precisely.

Exploring other potential abradable systems

The next step is to study one other composite system that possess the desired abradable properties and the chemical and thermal stability at high temperatures, for the hot section of IGCC turbines. Since all information regarding abradable coatings are proprietary in the turbine industry, choice of the systems would be based on the literature review and the anticipated potential of the materials (based on their properties) in the composites. The focus remaining on

the high temperature zone these materials must have ceramics as the basis. Two prominent systems under consideration are:

1) Layered structured LaPO4 added into 7 wt% yttria stabilized zirconia (7YSZ) as the soft phase (3) and
2) Air plasma sprayed ceramic double layer composed of 7YSZ as an intermediate layer and magnesia alumina spinel as a top layer (16).

The first candidate is 7 mol% YSZ integrated with Lanthanum Phosphate as a lubricating phase; $LaPO_4$ has been chosen because it has the potential of being high temperature thermal isolation material for its high melting point (2000 K), chemical stability and comparable conductivity than YSZ (1.5 W/mK). The thermal expansion coefficient is also close to the Zirconia based ceramics; and linear thermal expansion coefficient of LaPO4 is $9.69*10^{-6}$ K^{-1} at the range of 20-1000 ^{0}C and $11.19*10^{-6}$ K^{-1} for zirconia in the same temperature range. Previous studies have shown the co-existence of Zirconia and $LaPO_4$ at very high temperatures and they share weakly bonded interface which makes the system suitable for abradable applications at high temperature. The 9 fold structure of $LaPO_4$ is designed to make weak bonds with other oxides but forms very firm bond with other monazites; using this property of $LaPO_4$ it is used as the fracture surface which is supposed to deflect the cracks formed due to blade-coating interactions.

As YSZ has a high thermal expansion coefficient ($10–12.5 \times 10^{-6}$ K^{-1}) which is closer to the superalloy substrate materials ($>14 \times 10^{-6}$ K^{-1}) compared to other ceramics, they are the most widely used in high temperature coating applications. This leads to low stresses building up inside the coating during thermal cycling but in long-term applications, there are some restricting

factors for YSZ, such as its limited high-temperature capability. The surface temperature of Zirconia based layer exceeds maximum acceptable temperature for zirconium due to the fact that the self-insulation (~1.0 W/mK) property of zirconium oxide which leads to a large thermal gradient between the substrate and the surface. The tension in the outer layer and compression in the inner layer introduces vertical cracks which prompts delamination and coating failure. This ceramic system with alumina-rich magnesia alumina spinel has a lower thermal expansion coefficient ($\sim 9 \times 10^{-6}\ K^{-1}$) but higher Thermal conductivity ($\geq 2.0\ W/mK$), supposed to last longer since it never reaches the maximum acceptable temperature of spinel and the surface temperature remains way below than the Zirconia based coatings. Hence it is worthwhile to explore the dual layer ceramic coating system in high temperature humid environment.

BIBLIOGRAPHY

1. *Conditions in advanced turbines for IGCC power plants with carbon capture.* **White, B. M., Ames, R. W., & Burke, P.** s.l. : In ASME Turbo Expo 2013: Turbine Technical Conference and Exposition (pp. V002T03A005-V002T03A005). American Society of Mechanical Engineers., (2013, June). Proceedings of the ASME Turbo Expo.

2. *Control of coating properties of abradable seals by on-line process diagnostics.* **Lugscheider, E., Zwick, J., Hertter, M., & Sporer, D.** Basel, Switzerland. : In International Thermal Spray Conference (ITSC), 2005.

3. *Failure mechanisms of magnesia alumina spinel abradable coatings under thermal cyclic loading.* **Ebert, S., Mücke, R., Mack, D., Vaßen, R., Stöver, D., Wobst, T., & Gebhard, S.** s.l. : Journal of the European Ceramic Society, 2013, Vols. 33(15), 3335-3343.

4. *The wear mechanisms occurring in abradable seals of gas turbines.* **Borel, M. O., Nicoll, A. R., Schla, H. W., & Schmid, R. K.** s.l. : Surface and coatings technology, 1989, Vols. 39, 117-126.

5. *Friction and wear of several compressor gas-path seal materials.* **Bill, R. C., & Wisander, D. W.** s.l. : National Aeronautics and Space Administration, Scientific and Technical Information Office., 1978, Vol. Vol. 1128.

6. *Sealing in turbomachinery.* **Chupp, R. E., Hendricks, R. C., Lattime, S. B., & Steinetz, B. M.** s.l. : Journal of Propulsion and Power, March–April 2006, Journal of propulsion and Power, Vols. 22(2), 313-349.

7. *Process design and monitoring for plasma sprayed abradable coatings.* **Steinke, T., Mauer, G., Vaßen, R., Stöver, D., Roth-Fagaraseanu, D., & Hancock, M.** s.l. : Journal of thermal spray technology, 2010. 19(4), 756-764.

8. *Alternative methods for determination of composition and porosity in abradable materials.* **Matejícek, J., Kolman, B., Dubský, J., Neufuss, K., Hopkins, N., & Zwick, J.** s.l. : Materials characterization, 2006. 57(1), 17-29..

9. *Development of New Abradable/Abrasive Sealing Systems for Clearance Control in Gas Turbines.* **Scrinzi, E., Giovannetti, I., Sheng, N., & Leblanc, L.** s.l. : In ASME 2013 Turbine Blade Tip Symposium (pp. V001T05A004-V001T05A004). American Society of Mechanical Engineers, 2013, September.

10. *Thermal and chemical stability of hexagonal boron nitride (h-BN) nanoplatelets. .* **Kostoglou, N., Polychronopoulou, K., & Rebholz, C.** s.l. : Vacuum, 2015. 112, 42-45.

11. **Reeds, J. S.** *Introduction of the principles of ceramic processing.* 1988.

12. *A steady-state Bi-substrate technique for measurement of the thermal conductivity of ceramic coatings.* **Tan, J. C., Tsipas, S. A., Golosnoy, I. O., Curran, J. A., Paul, S., & Clyne, T. W.** s.l. : Surface and Coatings Technology, 2006. 201(3), 1414-1420..

13. *Measurement of interfacial shear mechanical properties in thermal barrier coating systems by a barb pullout method.* **Guo, S. Q., Mumm, D. R., Karlsson, A. M., & Kagawa, Y.** s.l. : Scripta Materialia, 2005. 53(9), 1043-1048..

14. *Analysis of a "barb test" for measuring the mixed-mode delamination toughness of coatings.* . **Liu, Y. F., Kagawa, Y., & Evans, A. G.** s.l. : Acta Materialia, 2008. 56(1), 43-49..

15. *Thermally sprayed abradable coating technology for sealing in gas turbines.* **By Scott Wilson, Oerlikon Metco AG, Wohlen, Switzerland.** s.l. : The Future of Gas Turbine Technology, 6th International Conference, 2012.

16. *Thermal conductivity and mechanical properties of YSZ/LaPO4 composites.* **Ren, X., Guo, S., Zhao, M., & Pan, W.** s.l. : Journal of Materials Science,, 2014. 49(5), 2243-2251..